# Ultra-low Field MRI for the Detection of Liquid Explosives Using SQUIDs

Michelle Espy, Mark Flynn, John Gomez, Christina Hanson, Robert Kraus, Per Magnelind, Karlene Maskaly, Andrei Matlashov, Shaun Newman, Tuba Owens, Mark Peters, Henrik Sandin, Igor Savukov, Larry Schultz, Algis Urbaitis, Petr Volegov, Vadim Zotev

Los Alamos National Laboratory, Applied Modern Physics Group, MS D454,
Los Alamos, NM 87545, USA. E-mail: espy@lanl.gov

***Abstract* – Recently it has become both possible and practical to perform MR at magnetic fields from μT to mT, the so-called ultra-low field (ULF) regime. SQUID sensor technology allows for ultra-sensitive detection while pulsed pre-polarizing fields greatly enhance signal. The instrumentation allows for unprecedented flexibility in signal acquisition sequences and simplified MRI instrumentation. Here we present the results for a new application of ULF MRI and relaxometry for the detection and characterization of liquids. We briefly describe the motivation and advantages of the ULF MR approach. We then present recent results from a 7-channel ULF MRI/relaxometer system constructed to non-invasively inspect liquids at a security check-point for the presence of hazardous material. The instrument was fielded to the Albuquerque International Airport in December, 2008, and results from that endeavor are also presented.**

Manuscript received March 25, 2009; accepted April 20, 2009. Reference No. ST-114; Category 4

***Keywords* – Nuclear magnetic resonance, NMR, low-field NMR, SQUID, security, explosive detection**

## I. INTRODUCTION

Nuclear magnetic resonance (NMR) and magnetic resonance imaging (MRI) are ubiquitous tools in science and medicine, providing powerful probes of local and macromolecular chemical structure and dynamics, as well as tomographic imaging. Because signal scales with magnetic field strength, the technological trend has been to higher and higher magnetic fields with Larmor precession frequencies of hundreds of MHz. Although high fields enhance magnetic resonance (MR) signal strength and many forms of image and spectral contrast, they also preclude or place significant restrictions on many potentially important applications. Recently it has become possible and practical to perform MR at much lower fields (from microtesla to millitesla), the so-called ultra-low field (ULF) regime; see for example [1], [2]. The draw-back of the method, the very low signal intensity can be mitigated by pre-polarization [3], [4] and the use of ultra-sensitive detectors such as SQUIDs. The simplified field generation allows flexibility in pulse sequences such as measurement field reversal and the ability to trivially change field strength. In contrast to conventional MRI, relative homogeneity of the measurement

field is not crucial, because microtesla-range magnetic fields of even modest relative homogeneity are highly homogeneous on the absolute scale [5]. Improvements in SQUID sensor technology allow ultra-sensitive detection in a pulsed field environment [6]. There are numerous additional advantages to the ULF MR approach including imaging in the presence of metals, open system design, enhanced $T_1$-weighted contrast [7] and strong magnetic relaxation dispersion exhibited by tissues in the μT – mT field range [8].

We have recently developed several applications of ULF MR including 46 μT imaging of the human brain concurrent with magnetoencephalography [9] [10]), possible ways for direct tomographic imaging of neural currents [11], and preliminary work in the determination of uranium enrichment fraction via relaxation and/or *J*-coupling [12], [13].

## II. AIRPORT SECURITY APLICATION: SCREENING

In airport security checkpoints, there is a strong desire to know the chemical content of materials being carried on board aircraft, but this determination must be made quickly and non-invasively. Since 2006, there has been increased concern about the threat of liquid explosives being carried on to aircraft, which has prompted costly and onerous travel restrictions on the volume of liquids passengers are allowed to carry on board.

Presently there are numerous screening technologies deployed and being tested at airport security check-points. However, most of these are looking for hidden weapons (x-ray and millimeter wave) or the presence of material residue from making bombs (mass spectrometry) and most of these methods focus on solids. X-ray is excellent for rapid and non-invasive screening of structure. Recently very sophisticated x-ray machines, such as [14], have been deployed that are able to distinguish liquids from solids. There is evidence that this approach might also be able to identify at least some threat liquids. However, accurate determination of a variety of threat liquids remains speculative. X-ray methods rely not on detection of chemical signature but on density and atomic number, which is more indirect. Moreover, the approach may have difficulties achieving sufficiently low alarm rates in case of complicated bottle shapes.

Mass spectrometry, which does give chemical structure, presently relies on either opening bottles up in the case of liquids, or swiping surfaces. Raman scattering, in which the frequencies and intensities of Raman-scattered photons reflect the conformation and electronic states of the probed molecule, can also provide a chemical signature. Electromagnetic methods based on multi-frequency microwave evanescent field sensors [15] measure the conductivity and dielectric relaxation of liquids, to provide a chemical fingerprint in a very short amount of time (~ 1 s). However, liquids in metal and metalized containers cannot be inspected by this technique. These approaches are all limited to single bottles, which makes luggage screening impractical. Single bottle approaches are more suitable for random checks. NQR or "zero field" NMR has been investigated for the detection of solid explosives, including SQUID-based approaches; see for example [16-20]. Thus far, none of these approaches has been widely fielded.

An important benefit of the MR approach is the ability to probe chemical structure. Indeed, MR spectroscopy is an ideal technology for screening liquids. However, conventional instrumentation, employing magnetic fields > 1T, presents an unacceptably large risk to the public. Presently, owing to lack of another screening technology, airport

rules require that all of a passenger's carry-on liquids be contained in 3-ounce bottles and that all of the bottles be placed in a single one-quart, zip-lock bag.

In this paper we present a ULF MR imager and relaxometer [21] known as "MagViz" that was designed for the non-invasive inspection of liquids at an airport security check-point. The MagViz system utilizes many of the advantages of ULF MR, in particular exploiting the power of relaxometry to fingerprint materials, the relatively simple MRI instrumentation suitable for a public setting, and the ability to image through non-ferrous metal foils and cans. While relaxometry is used to classify materials as "threat" or "benign", a low-resolution ULF MRI allows multiple bottles to be examined simultaneously and without opening. We show examples of performance, and report on this system's demonstration at the Albuquerque International Airport.

## III. PRINCIPLE AND APPROACH

Magnetic resonance imaging is an imaging modality used to construct images based on the NMR signal from the spin-polarized nuclei in an object. In medical MRI, radiologists are most interested in looking at the NMR signal from water and fat, the major hydrogen containing components of the human body. In the case of MagViz, we have also focused on the hydrogen in liquids, thus measuring the proton resonance. However, because the SQUIDs are operated as untuned detectors, other nuclei can be detected as well. The principle behind all magnetic resonance imaging is the resonance equation, which shows that the Larmor (resonance) frequency $\nu$ of a spin is proportional to the magnetic field, $B_o$, it is experiencing:

$$\nu = \gamma B_o .$$

The use of gradients allows for spatial encoding of the spins to produce an image; see for example [22]. In addition to imaging the bottles, MagViz must make a chemical identification of the material inside. At ULF it is not possible to resolve different spectral components in the frequency domain by chemical shift, and thus the technique exploits information in the time domain. Our approach to ULF spectroscopy relies on measurement of the relaxation parameters, $T_1$ and $T_2$, to provide information on the physical and chemical properties of the sample, an approach known as relaxometry. Relaxometry at low fields, ~ 0.1 T is frequently used in industrial applications where the instrumentation can be made quite simple with permanent magnets. MagViz operates as a ULF relaxometer for chemical identification. While the detectors are more complicated, due to the cryogenic cooling of the SQUIDs, the instrument has the advantages of very simple magnetic field generation hardware, low magnetic fields, low Larmor frequencies (at which signals can penetrate through metal cans, pipes, foil packaging), and enhanced contrast as described above.

Local magnetic field fluctuations, *e.g.*, due to particle motion, matching the spin Larmor frequency cause relaxation. The longitudinal or spin-lattice relaxation, $T_1$, involves redistributing the populations of the nuclear spin states to reach the thermal equilibrium distribution by energy exchange with their surroundings. The transverse or spin-spin relaxation, $T_2$, corresponds to decoherence of the transverse nuclear spin magnetization caused by random fluctuations of the local magnetic field [23]. The $T_1$

relaxation is generally strongly dependent on the measurement field strength. This is relevant for a ULF relaxometer approach where the polarization and measurement fields are independent in strength and orientation, and the measurement field can be easily varied to provide additional information [24].

## IV. INSTRUMENTATION AND EXAMPLES

The design of the MagViz instrumentation and the used field pulse sequence are shown schematically in Figure 1; these are similar to what has been described in [2, 25]. The MagViz system uses seven 2nd order wire-wound gradiometer pick-up coils, which are 90 mm in diameter; the baseline (coil separation along the gradiometer axis) is also 90mm. The arrangement of the gradiometers is shown in Figure 1(a). The gradiometer coils are connected to commercial CE2Blue SQUID sensors via cryogenic switches SW1 [26]. Cryogenic switches are activated during pre-polarization time and become normal with 350 Ohm resistance. The intrinsic noise of the gradiometers and the commercial cryostat [27] is only about 0.5 fT/√Hz. However, external noise sources increase the total system noise at measurement frequency up to the 1.5-2 fT/√Hz level. Such noise sources include the gold-plated radio frequency interference shield around the cryostat, the measurement field and gradient electronics, feedback electronic components etc.

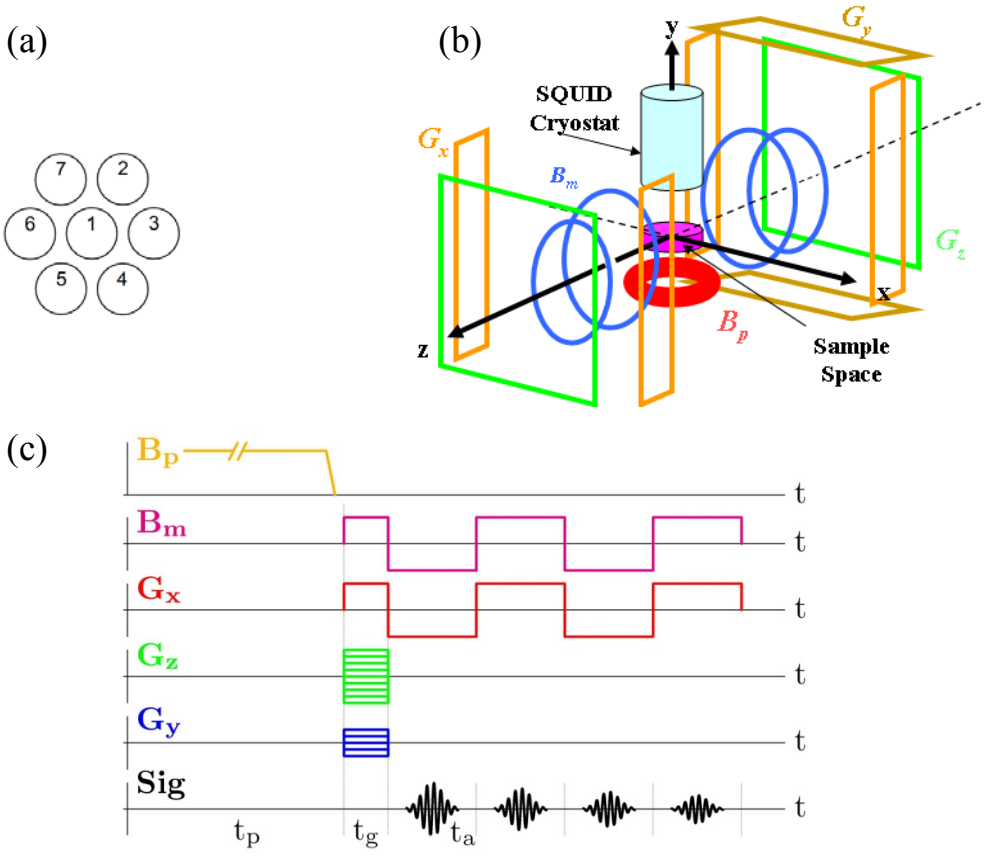


**Fig. 1.** (a) Arrangement of the 7 SQUID gradiometers. (b) Magnetic field generation coils. One set of $G_z$ gradient coils is not shown for clarity. (c) Pulse sequence.

Figure 1(b) shows the arrangement of magnetic field generation coils. The pre-polarization coil, generating the field $B_p$, is cooled by a fluorine-based industrial coolant, Fluorinert™, allowing continuous running without substantial heating. Fluorine was

**Fig. 2.** Photograph of the inside of the MagViz system.

chosen instead of water for cooling to avoid hydrogen background. We do see the 19F signal from the coil itself, but this appears at a frequency removed from our area of interest ($\gamma$ = 42.6 MHz/T for protons and 40.0 MHz/T for 19F). The $B_p$ coil has 0.34 H inductance and it is capable of attaining prepolarization fields as high as 50 mT in a sample volume at 35 A current. After some pre-polarization time (ranging from 1-3 seconds) the $B_p$ field is turned off non-adiabatically (with a ramp-down time of 10 milliseconds) and the much weaker measurement field, $B_m$, is applied perpendicular to $B_p$ to start precession. The intensity of $B_m$ typically ranges from 50 to100 μT (proton Larmor frequencies from ~2kHz to 4kHz). A measurement field echo technique is used to reduce the effects of magnetic field inhomogeneity. The measuring field and gradient sequence is shown in Figure 1(c). Such a sequence would be impossible with a conventional MRI system where the measurement field is generated by large permanent or superconducting magnets with fixed field orientations. Gradient field echoes in the *x*-direction are also used. The encoding scheme is based on the 3D Fourier protocol with a frequency encoding gradient $G_x = dB_z/dx$ and two phase encoding gradients, $G_z = dB_z/dz$ and $G_y = dB_z/dy$ [2, 28]. The following imaging parameters were used in the present work: $G_x$ = ±60 μT/m, $|G_z| \leq 24$ μT/m, 9 encoding steps, $|G_y| \leq 7$ μT/m, 3 steps, polarization time $t_p$ =

1 s and 3 s, gradient encoding $t_g$ = 50 ms, and acquisition $t_a$ = 85 ms The lowest sequence is that of the NMR echo signal. The actual MagViz hardware is shown in Figure 2.

From the sequence described above we determine $T_2$ and a low- resolution image, 5 mm x 10 mm x 30 mm, is produced. The measurement of $T_2$ is performed at a lower field value $B_m$. However, $T_1$ is determined by repeating the pulse sequence shown in Figure 1(c) for two differing polarization times, $t_p$ and using a higher (50 mT) pre-polarization field. The spins are allowed to reach their thermal equilibrium distribution in the polarization field for $t_p \sim 1$ s in the first sequence applied, and then the entire procedure it is repeated with $t_p \sim 3$ s. The difference in the measured signal amplitude between the two polarizing times, $t_p$, is then used to determine the value of $T_1$. Such combination of relaxation parameters provides robust parameter space for classification of liquids. To minimize effects of the residual fields and non-uniformity of the measurement field, polarity of the both fields (*i.e.*, of the polarization field and measurement field) is alternated from scan to scan, and the measurement field from echo to echo. To minimize the measurement time the SENSE technique is used [29].

Prior to data collection the system is calibrated with a uniform water phantom consisting of a cylinder ~ 250 mm in diameter and 75 mm deep. Using the phantom, the SQUID sensors' sensitivity maps are obtained for each polarity of the polarization field and each echo. Subsequent images are reconstructed relative to the water calibration. Such an approach also compensates for the effects of any static residual fields, thus improving estimation of the transversal relaxation time. The reconstructed relaxation maps are combined into a pseudo-color image (Figure 3, rows (b) and (c)), which visualizes relaxation properties of the samples and alerts an operator if a controlled substance is present. To automatically classify the samples, the reconstructed images are segmented using a multi-dimensional mean-shift algorithm [30] and the computed

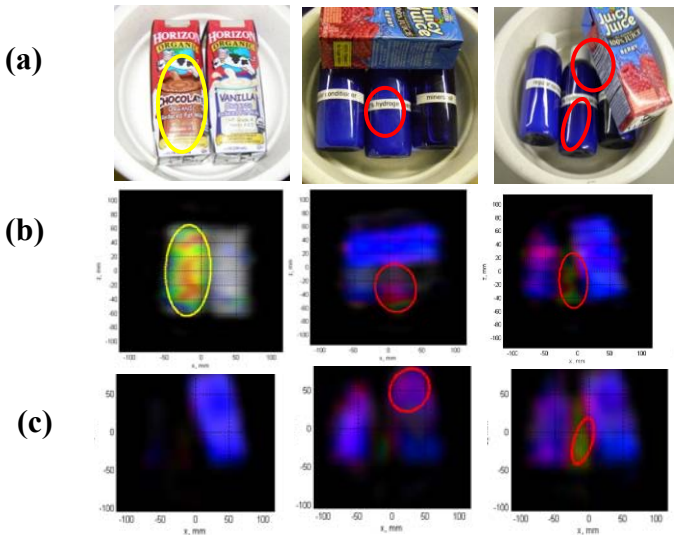


**Fig. 3.** Row (a): photographs of items. (b): 2-D images with threat detection. (c): 3-D slices through the items shown in row (a), far right.

relaxation parameters of the detected objects are compared against database entries. The method is capable of classification of multiple samples in random configurations, to depths up to ~ 100 mm. Figure 3 shows several samples in 2- and 3-dimensional imaging

protocols, with threats identified. The time to acquire the images shown was 45 s for 2D and 75 s for 3D. Tests were performed with benign items from streams of commerce, and a threat material, hydrogen peroxide. The 2D analysis integrated over the depth of the bowl, which was ~ 75 mm. The 3D analysis is shown with three slices. Red and yellow ovals indicate correctly identified objects containing threat material. In the upper left, material hidden in a foil-lined box was correctly identified. The unit was also used to analyze the difference between several different types of liquors. These data are presented in Table I, where the tolerances indicate measurement uncertainty.

**Table I.** Relaxation values for liquors measured in MagViz.

| Substance | $T_1$ (mSec) | $T_2$ (mSec) |
|---|---|---|
| Wine #1 shiraz | 880 ± 40 | 590 ± 10 |
| Wine #2 chardonnay | 1100 ± 40 | 780 ± 10 |
| Wine #3 shiraz | 1050 ± 40 | 700 ± 40 |
| Whiskey | 1410 ± 40 | 1230 ± 10 |
| Brandy | 1600 ± 40 | 1340 ± 10 |

## V. THE SYSTEM AND ITS AIRPORT DEMONSTRATION

In December of 2008 the MagViz system was demonstrated in the field, at the Albuquerque International Airport. Thus, in addition to the challenges of making a functional ULF MRI instrument for laboratory research, we also had to adapt the system for a small, mobile magnetically shielded enclosure (height 2 meters, width 1.8 m, depth 1.55 m) [31], develop a "noise free" conveyor system through the shield for sample handling, and making the instrument easy to assemble and disassemble. In addition there were minor logistical tasks such as performing liquid helium cryogenic transfers in the airport.

The primary challenge of the small shielded enclosure was to suppress transients induced in the mu-metal during the pre-polarization field cycling, and the magnetization of the enclosure. Neither of these are issues in the large MEG-style shielded enclosures our ULF MR systems typically operate in, as the walls are much farther away. To compensate for the transients after pulsing, external low-frequency negative feedback was implemented. To compensate for effects due to magnetization of the shield, we adopted the strategy of reversing the orientation of the pre-polarization field from scan to scan, as described above.

The conveyor system consisted of three parts, entry, assay, and exit. The entry and exit conveyors were off-the shelf and the assay section was entirely made of non-magnetic materials. Mu-metal doors controlled by air pressure were used to complete the enclosure's shield after the sample entered the assay area. The mu-metal enclosure itself could be mounted on wheels. The entire coil set was an independent unit that could be

slid in and out of the enclosure for transport. The entire shield and field generation assembly could be disassembled and reassembled in a single day. The MagViz system operated in the Albuquerque airport for approximately two weeks. In that time the system scanned items that were confiscated from the security check-point for exceeding the 3 ounce limit. Hundreds of items from streams of commerce were scanned, with most being water bottles. No hazardous items were found. Figure 4 shows the photograph of the system assembly at the airport (right) and an artist's conception drawing showing the cryostat and the coil assembly within the shielded enclosure. MagViz successfully detected threat material hidden in carry-on travel kits and foil lined drink boxes. Figure 5 shows photographs taken during the operation at the Albuquerque airport: the placing of samples on the conveyor by the operator (left) and a snapshot of the operator's laptop screen showing detection of threat material. After the demonstration, the system has returned to Los Alamos National Laboratory where it is being used for further database development and basic research on the relaxation properties of materials.

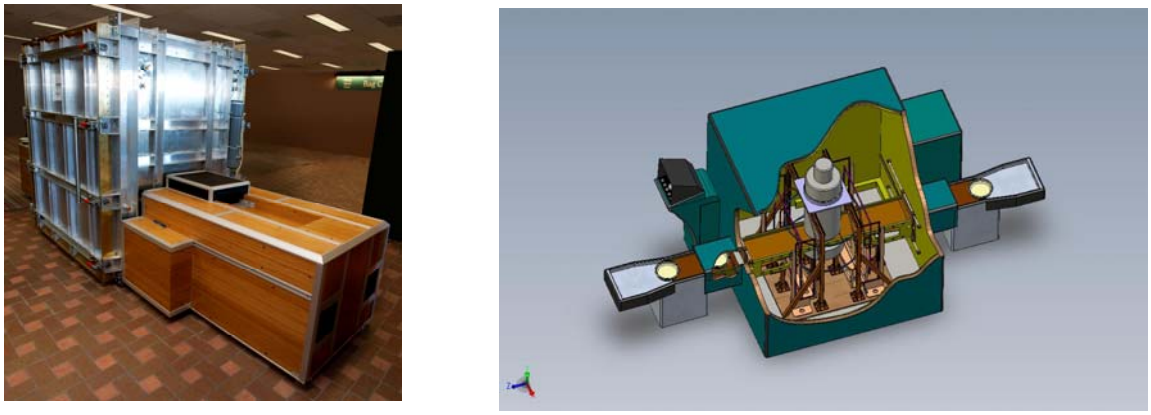

**Fig. 4.** The system photo at the airport (left), and a conceptual drawing showing the cryostat and coils within the shielded enclosure (right).


**Fig. 5**. Photos from actual operation: on the left samples being placed onto the conveyor. On the right a laptop screen shot showing detection of threat (red) material

## VI. FUTURE WORK

Thus far the MagViz project has focused on high concentration (> 40% by volume) hydrogen peroxide, which is an oxidizer commonly used for improvised liquid explosives. Hydrogen peroxide is a substance expected to be difficult to detect since the chemical structure ($H_2O_2$) is very close to that of water. Now that the proof-of-concept has been demonstrated, a major objective of the project is to add other materials to the database. The Department of Homeland Security maintains a list of nearly 100 items including oxidzers, fuels, and mixtures that should be excluded from airplanes. These all need to be measured and characterized. Preliminary results indicate that MagViz can also distinguish certain fuels; however this needs to be investigated further. Moreover, we have only scanned between 100 and 200 items from streams of commerce. While the false-positive rate presently is acceptably low (less than a few percent), obviously there are many more types of items carried aboard aircraft. Although we have not observed any significant effect of bottle shape or configuration of bottles on accuracy (other than those related to signal-to-noise for very small bottles or bottles at a depth greater than 100 mm) we need to rigorously study possible effects.

Ultimately, the $T_1$ and $T_2$ properties of different liquids provide a two dimensional parameter space, representing physical parameters of the liquid which are connected to the chemical composition, in which regions for benign and harmful liquids need to be clearly separated. Determining whether or not this is possible will be a significant focus of future work.

At the same time, throughput is a critical consideration. Even for segregated liquids the MagViz scan time is still unacceptably long for a primary screening tool. The desired scan speed is < 15 s, as with X-ray scanning, while MagViz scan times are 60 s at present. Nevertheless, even at these speeds it may be suitable for secondary or specialized screening. What limits the scan time are the many steps required for imaging. We are investigating whether or not MagViz instrumentation could be combined with a faster imaging method like the advanced x-ray systems capable of determining the presence of liquids, so that scans can be limited to known areas of interest. Ultimately, the goal is for screening without the need for segregating liquids. However, this will be limited by our ability to scan in the presence of the magnetic material, which will invariably be found in suitcases. This is an extremely challenging area for study. The ability of MagViz to reliably detect a variety of threats, in a practical configuration and with reasonable screening times, is a critical consideration for determining how useful a screening tool it will ultimately be.

## VII. CONCLUSIONS

The MagViz system was a direct spin-off from research in the human brain [9]. Our experience is the classic story of basic science being leveraged in an unexpected way. While we remain very enthusiastic about the potential of MagViz-like systems for airport security, we believe the real potential of mobile ULF MRI may extend greatly beyond this application, or others we are presently exploring. A simple, mobile, inexpensive MRI system like MagViz could open up many markets for MRI. For example, because of the

high cost of magnets (permanent or superconducting) many people in resource-poor locations do not have access to MRI. Moreover, the ULF MR approach may provide MRI systems for emergency or battlefield medicine. Without any hardware modification at all, the MagViz system is a capable imaging device. In Figure 6 we show a two dimensional MRI scan of human knees taken in the MagViz unit. The scan time for the image presented was ~ 30 minutes. While the spatial resolution remains below that of conventional MRI devices we expect this to improve as our ability to increase the pre-polarization fields and reduce system noise improves. The female subject was scanned in normal street clothing, and was wearing glasses and jewelry during the scan.

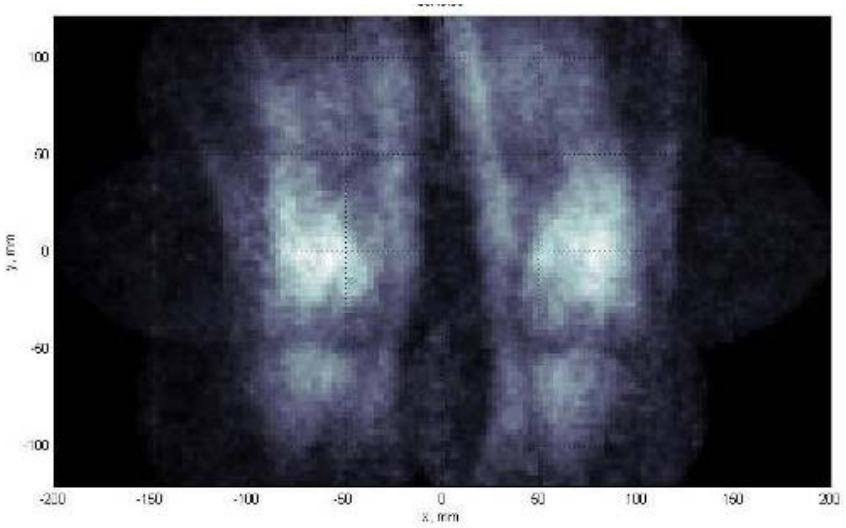


**Fig. 6.** MRI scan of human knees acquired in the MagViz instrument.

The real potential of the method as a scientific tool remains to be determined. While some relaxation mechanisms are already understood and experimentally verified at high field, relaxation behavior at ULF has not been rigorously studied experimentally or theoretically. ULF MR provides a tool to study relaxation *versus* frequency to characterize relaxation behavior and hence the underlying molecular dynamics. One of the most promising applications of ULF MR is the study of the "slow" dynamic processes. Enhanced relaxation contrast in biological tissue, a unique benefit of imaging at ULF, is presumably the result of these complicated motions. Yet the theory of MR relaxation, which provides a window into these dynamics, has not been developed and validated below 10 kHz. The frequency dependence of relaxation at ULF may provide an exciting probe for molecular dynamics on the millisecond timescale relevant to a host of applications yet to be explored.

## ACKNOWLEDGEMENTS

The authors gratefully acknowledge the support of this work by the U.S. Department of Homeland Security. We also thank Michael Borden for organizing the engineering effort required to realize the MagViz instrumentation. The authors appreciate the constructive comments by Dr. Norbert Klein (FZ-Jülich and EMISENS) on the content of this paper.

## REFERENCES


[1] R. McDermott, S-K. Lee, B. ten Haken et al., "Microtesla MRI with a superconducting quantum interference device", *Proc. Natl. Acad. Sci. USA* **101** 7857-7861 (2004).

[2] V. S. Zotev, A. N. Matashov, P. Volegov et al., "SQUID-based instrumentation for ultralow-field MRI", *Supercond. Sci. Technol.* **20**, S367-S373 (2007).

[3] M. Packard, R. Varian, "Free nuclear induction in the earth's magnetic field", *Phys. Rev.,* **A93,** 941, (1954)

[4] A. Macovski, S. Conolly, "Novel approaches to low-cost MRI", *Mag. Res. Med*. **30**, 221-230 (1993).

[5] R. McDermott, S. Lee, B. ten Haken et al., Liquid-state NMR and scalar couplings in microtesla magnetic fields, Science 295 (2002) 2247-2249.

[6] V. Zotev, A. N. Matlashov, P. Volegov et al., "Multi-Channel SQUID System for MEG and Ultra-Low Field MRI", *IEEE Trans Supercond.,* **17**(2), 839-842 (2007)

[7] S. K. Lee M. Mössle, W, Myers et al., "SQUID-detected MRI at 132 μT with $T_1$-weighted contrast established at 10 μT-300 mT", *Magn. Res. Med*. **53**, 9-14 (2005).

[8] S. H. Koenig, R. D. Brown, "Field-cycling relaxometry of protein solutions and tissue: implications for MRI", *Progr. NMR Spectrosc*. **22**, 487-567 (1990).

[9] V. S. Zotev. A. N. Matlashov, P. Volegov et al., "Microtesla MRI combined with MEG", *J. Mag. Res.* **194** (1) , 115-120 (2008).

[10] V. S. Zotev, A. N. Matlashov, P. L. Volegov et al., "Microtesla MRI of the human brain combined with MEG", *Eur. Supercond. News Forum*, No. 4, April 2008, http://www.ewh.ieee.org/tc/csc/europe/newsforum/pdf/ST31_brainFinal_020708.pdf

[11] R. Kraus, P. Volegov, A. Matlachov, M. Espy, "Toward Direct Neural Current Imaging by Resonant Mechanisms at Ultra-Low Field", *Neuroimage* **39**, 310- 317 (2008).

[12] P. Volegov, A. Matlashov, R. H. Kraus, "Ultra-low field NMR measurements of liquids and gases with short relaxation times", *J. Mag. Res.* **183**, 134–141 (2006).

[13] P. Magnelind, A. Matlashov, P. Volegov, M. Espy, "Ultra-low Field NMR of $UF_6$ for $^{235}U$ Detection and Characterization", *IEEE Trans. Appl., Supercond*., *accepted for publication*.

[14] *Smith's HI-SCAN 6040aTiX,* 64 Clarendon Road, Watford, Herts WD17 1DA, UK.

[15] EMISENS GmbH, Karl-Heinz-Beckurts Str. 13, D-52428 Jülich, info@emisens.de

[16] N. Q. Fan, J. Clarke, "Low-frequency nuclear magnetic resonance and nuclear quadrupole resonance spectrometer based on a DC superconducting quantum interference device" *Rev. Sci. Instrum.* **62** 1453–9 (1991).

[17] J. P. Yesinowski, M. L. Buess, A. N. Garroway, "Detection of N-14 and Cl-35 in cocaine base and hydrochloride using NQR, NMR and SQUID techniques", *Anal. Chem.* **67** 2256–63 (1992).

[18] D. M. Tonthat, J. Clarke, "Direct current superconducting quantum interference device spectrometer for pulsed nuclear magnetic resonance and nuclear quadrupole resonance at frequencies up to 5 MHz", *Rev. Sci. Instrum.* **67** 2890–3 (1996).

[19] D. F. He, M. Tachiki, H, Itozaki, "N-14 NQR using a high-Tc rf SQUID with a normal metal transformer", *Supercond. Sci. Technol.* **21,** 015023 (4pp) (2008).

[20] A. N. Garroway, M. L. Buess, J. B. Miller et al., "Remote Sensing by Nuclear Quadrupole Resonance", *IEEE Transactions on Geoscience and Remote Sensing*, **39** (6), (2001).

[21] M. Espy, M. Flynn, J. Gomez et al., "Applications of Ultra-low Field Magnetic Resonance for Imaging and Materials Studies", *IEEE Trans. Appl. Supercond.*, *accepted for publication*..

[22] E. M. Haacke, R. W. Brown, Thompson M. R, Venkatesan R., "Magnetic resonance imaging: physical principles and sequence design" *Wiley-Liss New York* (1999).

[23] R. Kimmic, E. Anoardo, "Field-cycling NMR relaxometry" *Prog. Nucl. Mag. Res. Spect*., **44**, 257-320 (2004).

[24] G. J. Bene, "Nuclear magnetism of liquid systems in the Earth field-range*", Phys. Rep.* **58** (4), 213–267 (1980).

[25] V. S. Zotev, A. N. Matlashov, P. Volegov et al. "Multi-channel SQUID system for MEG and ultra-low-field MRI", *IEEE Trans. Appl. Supercond*. **17** 839-842 (2007).

[26] SUPRACON AG, http://www.supracon.com

[27] CRYOTON Co. Ltd., http://cryoton.webzone.ru

[28] V. Zotev, P. Volegov, A. Matlashov et al., "Parallel MRI at microtesla fields", *J. Magn. Reson.* **192,** 197-208 (2008).
[29] K. P. Pruessmann, M. Weigner, M. B. Sheidegger et al., "SENSE: Sensitivity Encoding for Fast MRI", *Magnetic Resonance in Medicine* **42**, 952-962 (1999).
[30] B. Georgescu, I. Shimshoni, P. Meer, "Mean Shift Based Clustering in High Dimensions: A Texture Classification example" *Proc ninth Int'l Conf. Computer Vision.* 456-463 (2003).
[31] IMEDCO, http://www.imedco-shielding.com/englisch/intro.html